



# Shape memory polymer variable stiffness magnetic catheters with hybrid stiffness control

## Conference Paper

### Author(s):

Mattmann, Michael; [Boehler, Quentin](#) ; Chen, Xiang-Zhong; Pané, Salvador; [Nelson, Bradley](#) 

### Publication date:

2022-10-23

### Permanent link:

<https://doi.org/10.3929/ethz-b-000588302>

### Rights / license:

[In Copyright - Non-Commercial Use Permitted](#)

### Originally published in:

<https://doi.org/10.1109/IROS47612.2022.9981935>

### Funding acknowledgement:

185039 - Arbeitstitel "Soft Magnetic Robots: Modeling, Design and Control of Magnetically Guided Continuum Manipulators" (SNF)

743217 - Soft Micro Robotics (EC)

771565C - Highly Integrated Nanoscale Robots for Targeted Delivery to the Central Nervous System (EC)

# Shape memory polymer variable stiffness magnetic catheters with hybrid stiffness control

Michael Mattmann, Quentin Boehler, Xiang-Zhong Chen, Salvador Pané, Bradley J. Nelson

**Abstract**—Variable stiffness catheters typically rely on thermally induced stiffness transitions with a transition temperature above body temperature. This imposes considerable safety limitations for medical applications. In this work, we present a variable stiffness catheter using a hybrid control strategy capable of actively heating and actively cooling the catheter material. The proposed catheter is made of a single biocompatible shape memory polymer, which significantly increases its manufacturability and scalability compared to existing designs. Potentially increased safety is obtained by ensuring a lower-risk compliant state at body temperature while maintaining higher stiffness ranges in actively controlled states. Additionally, the combined use of variable stiffness and magnetic actuation increases the dexterity and steerability of the device compared to existing robotic tools.

## I. INTRODUCTION

Soft continuum robots have become a key component in minimally invasive medicine. Robotic catheters and endoscopes have demonstrated their advantages in multiple medical fields showing increased precision, better outcomes, reduced recovery time, and a reduction in the physical and mental impact on surgeons [1]–[7]. Four-dimensional (4D) soft robots [8], [9] have recently proven their ability to overcome the fixed stiffness limitations of conventional surgical tools. Variable stiffness (VS) technologies, such as 4D robots, allow the surgeons to modify the tool stiffness, enabling precise control of the forces applied to the surrounding tissue [10]. The compliance, in the flexible configuration, guarantees safe navigation without the risk of tissue damage. At the same time, the ability to increase the stiffness allows matching the clinical needs when a contact force, gripping action, or support is required [11]–[16]. Cardiac ablation catheters, for instance, must maintain sufficient but safe contact force between the catheter and the heart wall, while allowing safe and precise steering.

The use of remote magnetic navigation (RMN) to control magnetic continuum robots provides excellent steerability and controllability and avoids the integration of pull wires, therefore contributing to the overall miniaturization of soft robotic tools [17]. The use of VS technology for magnetically guided catheters is of particular interest as it provides a larger and more dexterous workspace compared to conventional magnetic tools [7], [10], [18], [19]. It also allows

the use of multiple tools simultaneously [20]. Despite the advantages of VS technology, scalable approaches are still limited to thermally induced stiffness transitions [15], [18], [21]–[25]. Our group has recently developed two scalable VS technologies that rely on a low melting point alloy (LMPA) and a composite shape memory polymer (SMP) [10], [20], [25], resulting in the smallest magnetically steerable variable stiffness catheters (VSC) to date. However, both technologies pose considerable safety issues, as a failure in the heating system presents a risk to the patient that must be considered. For example, the dependence on active heating to reach a compliant state can lead to a difficult or impossible retrieval of the tool in the case of a heating and control system failure. Additionally, heating only catheters rely on temperatures larger than 37°C to achieve a transition from the rigid to the flexible state. Medical applications do however prevent the use of surface temperatures larger than 41°C for endovascular interventions or 51°C for endoscopic applications. This limits the material choice, prevents the use of the full stiffness range, and increases the complexity of VS tools as additional insulation layers are required. A VSC with a transition temperature below the body temperature and active cooling capabilities would therefore significantly increase safety, broaden the material choice, and increase the field of applications. Cooling based technologies are, however, still restricted to larger scales (> 10mm), as additional cooling and control structures need to be incorporated into the VSC [22], [26], [27]. This poor scalability limits the use of these devices to endoscopic procedures, and prevents their application in endovascular procedures where tool diameters are usually below 3 mm. Additionally, cooling only technologies still rely on passive temperature control and show a slow and asymmetric stiffness transition. A hybrid stiffness control, with both heating and cooling, overcomes the need for passive temperature control, therefore, overcoming the asymmetric behavior in stiffness transition reported in all thermally induced VSC and generally increases the transition speed between the stiffness states. These improvements greatly benefit practical applications by avoiding undesired waiting times.

Here, we propose a new VS technology that relies on a thermoset SMP with embedded cooling and control structures. The device exploits the advantages of SMPs reported in our previous work [20], and allows for the integration of control and cooling structures without additional elements. By avoiding additional embedded elements, we provide a technology that further miniaturizes safe VS tools with a transition temperature below body temperature. The pro-

This work was supported by the Swiss National Science Foundation through grant numbers 200020B-185039, and the ERC Advanced Grant 743217 Soft Micro Robotics (SOMBOT).

Michael Mattmann, Quentin Boehler, Xiang-Zhong Chen, Salvador Pané, and Bradley Nelson, are with the Multi-Scale Robotics Lab, ETH Zürich, Zürich CH-8092, Switzerland (e-mail: [michaema@ethz.ch](mailto:michaema@ethz.ch), [qboehler@ethz.ch](mailto:qboehler@ethz.ch), [chenxian@ethz.ch](mailto:chenxian@ethz.ch), [vidalp@ethz.ch](mailto:vidalp@ethz.ch), [bnelson@ethz.ch](mailto:bnelson@ethz.ch))

posed robotic system can be easily manipulated in open volumes and guarantees fast switching between the soft and rigid states. The introduction of hybrid stiffness control with the ability to both heat and cool in 4-dimensional soft robotics extends the range of medical procedures that can be executed with minimally invasive approaches and increases the attractiveness of variable stiffness technologies in fields with scalability and transition speed restrictions.

## II. MATERIALS AND METHODS

### A. Variable stiffness catheter

We select an SMP as the VS material because of its tunable transition temperature and the ability to transition between a glassy and rubbery state. These properties allow for a VSC with a glass transition temperature below body temperature with integrated heating and cooling structures, thereby avoiding additional elements. Fig. 1 illustrates the proposed design. The catheter consists of an SMP body (NOA63, Norland Prod.) with embedded heating, cooling, and measurement elements. Enamelled copper wires are used as heating and measurement elements using, respectively, joule heating and the resistivity change upon temperature change. The coiled design has been chosen to maximize the wire length, therefore providing a high measurement signal and homogeneous heating.

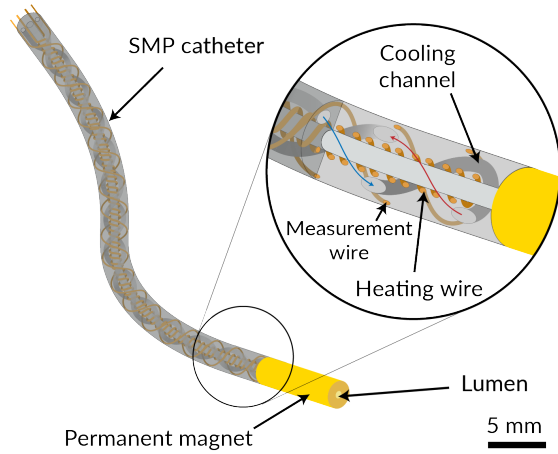


Fig. 1. Schematic illustration of the variable stiffness catheter. The shape memory polymer body encapsulates an inner lumen for tool insertion or drug injection, a cooling channel, heating wires, and measurement wires. The permanent magnet at the tip enables remote magnetic actuation.

Pumping cold water through the embedded channels allows them to act as cooling elements. The designed catheter has an outer diameter (OD) of 2.5mm and an inner lumen diameter (ID) of 0.5mm that can be used for the insertion of tools, electrical signal transmission, or drug injection. A permanent magnet is positioned at the catheter's tip, enabling magnetic actuation.

### B. Fabrication

The fabrication of the VSC relies on two molding steps as illustrated in Fig. 2a. In the first step, the heating wire is

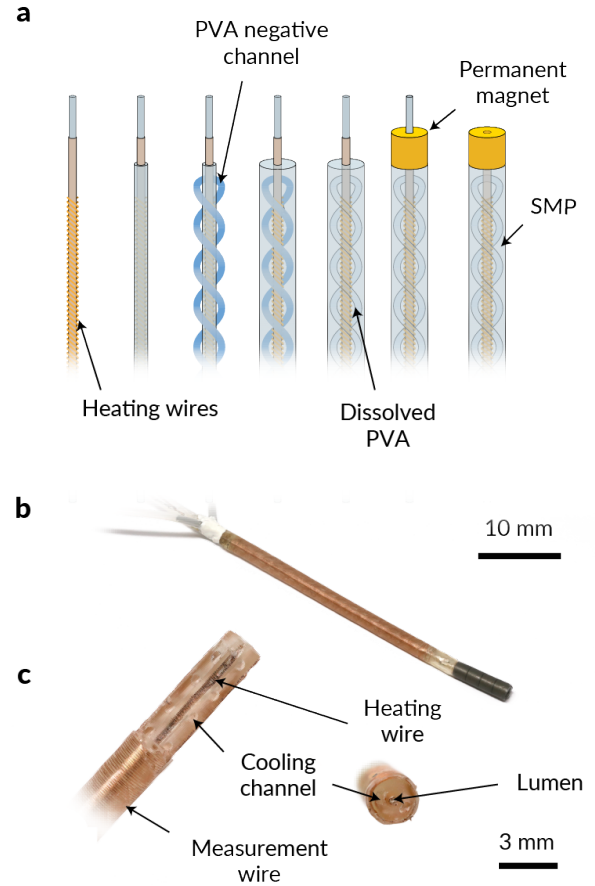


Fig. 2. Manufacturing of the variable stiffness catheter (VSC) and the obtained prototypes. a) Fabrication of the VSC. The heating wire is coiled around a Polytetrafluoroethylene (PTFE) liner and coated with a first layer of NOA. The negative cooling channels are positioned on top of the obtained structure and NOA is injected into the surrounding space. The Polyvinyl alcohol (PVA) structure is dissolved in a heated ultrasonic bath and the permanent magnet is glued onto the catheter tip. Finally, the central mandrel is removed leaving the catheter lumen. b) Picture of a VSC with electrical and cooling connections on the back. c) Parallel and perpendicular cross-sections of the catheter illustrating the embedded structures.

coiled around the inner Polytetrafluoroethylene (PTFE) liner and a first SMP layer is molded, in a straight configuration, on the surface. Next, the polymer layer is cured under UV-A light for 30 minutes and the structure is subsequently used to position the Polyvinyl alcohol (PVA) structure, which acts as a negative template for the cooling channels. An Ender-3 3D printer (Creality 3D) was used to extrude the negative PVA structure. The structure is obtained by extruding a PVA filament onto a rotating steel rod while controlling the nozzle linear velocity, the extrusion speed, and the rotational velocity of the steel rod. Next, the second SMP layer is molded on the PVA structure, which is subsequently dissolved in a heated ultrasonic bath, leaving the embedded cooling channels. Finally, the measurement wires are wound onto the outer surface of the catheter and the permanent magnet is glued onto the catheter tip with an additional drop of SMP. The finished catheter is shown in Fig. 2b. The

VS segment has a length of 50mm and is placed between the permanent magnet and the connections on the back. Fig. 2c shows two cross-section perspectives to visualize the embedded heating, cooling, and measurement structures.

### C. Cooling structure

The design of the cooling structure must address several conflicting design parameters. First, the catheter surface should be homogeneously cooled below the glass transition temperature to ensure full stiffness recovery upon cooling. The volume of VS material should also be maximized to

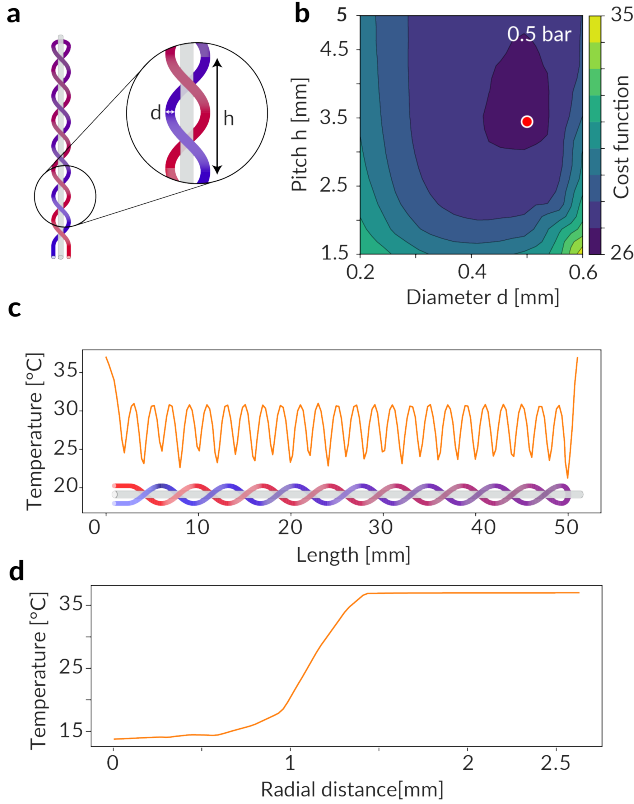


Fig. 3. Optimization of the cooling structure. a) Illustration of the cooling structure design with design parameters. b) Optimization graph for a relative cooling inlet pressure of 0.5 bar. c) Temperature along the cooled catheter, 0.1 mm below the surface. d) Average radial temperature profile of the cooled VSC.

ensure maximum stiffness variation. Finally, the surface temperature should be homogeneous and symmetric to prevent asymmetries during magnetic actuation. To meet these requirements, we chose a design relying on a double helix structure with the cold-water inlet on one helix and the outflow on the other. This design guarantees a symmetric temperature distribution and sufficient cooling in the entire geometry. A numerical parametric sweep on the channel diameter and pitch was performed using COMSOL Multiphysics to define the optimum design (pitch and diameter of the cooling channel) minimizing the surface temperature and volume loss. Fig. 3a illustrates the design parameters. The catheter dimensions were fixed with an OD of 2.5 mm, an ID of 0.5 mm, and a major helix pitch of 0.75 mm.

The parameters were optimized according to Equation 1, with  $T$  being the average surface temperature at a radial depth of  $100\mu\text{m}$ ,  $T_{min}$  the lowest possible temperature,  $V_{max}$  the catheter volume without cooling channels, and  $V$  the total catheter volume. The cost function has been chosen to equally weight the volume loss and temperature deviation from  $T_{min}$ .

$$cost = (T - T_{min}) + (V_{max} - V)/5.5 \quad (1)$$

Numerical optimization was performed assuming the catheter is positioned centrally in the aortic blood flow with an aortic diameter of 20 mm, a flow velocity of 1.2 m/s, and a flow temperature of  $37^\circ\text{C}$ . The obtained result for a relative cooling inflow pressure of 0.5 bar is displayed in Fig. 3b. We observed an optimal design, minimizing the cost function, with a channel diameter of 0.5 mm and a channel pitch of 3.5 mm. Fig. 3e-f show the simulated temperature along the catheter length and the radial temperature profile for a catheter positioned in the aortic blood flow ( $37^\circ\text{C}$ , 1.2 m/s) with the optimized design parameters. The temperature,  $100\mu\text{m}$  below the surface, oscillates between  $24^\circ\text{C}$  and  $32^\circ\text{C}$  with an average of  $27.5^\circ\text{C}$ . From the radial temperature profile, we observed that the material temperature was, on average, below the glass transition temperature ( $30^\circ\text{C}$ ) for all radii smaller than 1.15 mm. In the modeled environment, the heat removed by the cooling structures amounted to 3.3 W.

### D. Hybrid stiffness control

Fig. 4 shows the relationship between the materials elastic modulus and temperature. To ensure control on the full stiffness range, the temperature of the catheter needs to be controlled between  $5^\circ\text{C}$  and  $51^\circ\text{C}$ . Given the linear relationship between measurement wire resistance and surface temperature (Fig. 5a), the resistance is used as a direct feedback on the tool temperature and stiffness. Fig. 6a

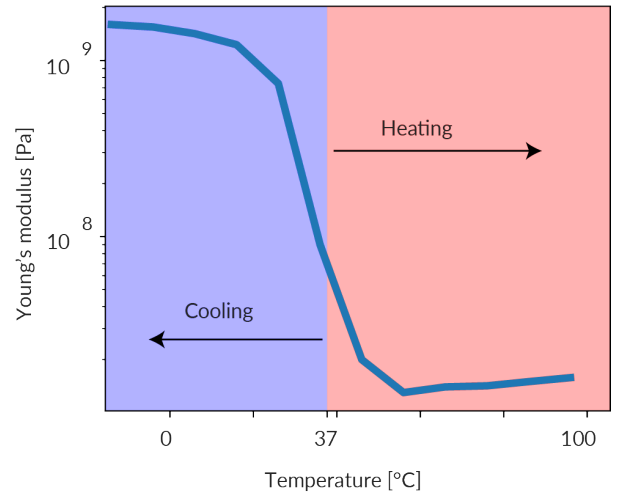


Fig. 4. Elastic modulus of NOA63 over bulk temperature. The blue range indicates where cooling is required, while the red range indicates the requirement for heating.

schematically shows the control setup consisting of a closed loop water circuit and a heating loop. A cold plate provides cold water at a constant temperature of 5°C. The pump speed and heating current are controlled with motor drives (DRV8871 DC Motor Driver, Adafruit) and a microcontroller (Arduino Uno). Fig. 6b illustrates the design of the stiffness control. The surface temperature is evaluated by measuring the resistance of a copper wire positioned on the catheter surface. The thermal coefficient  $\alpha$  was measured with the following linear approximation (Fig. 5a) with  $\rho$  the resistivity and  $\rho_0$  the resistivity at  $T_0$ .

$$\rho(T) = \rho_0 \cdot (1 + \alpha(T - T_0)) \quad (2)$$

The measured temperature is used to evaluate whether

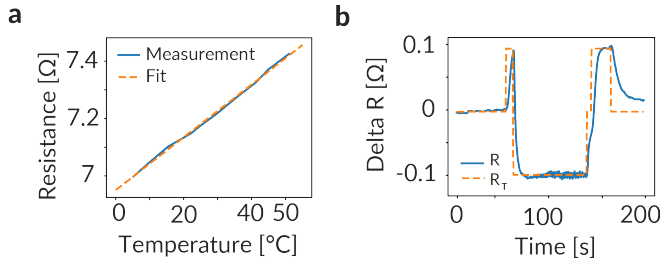


Fig. 5. Controller characteristics. a) Linear relationship between the resistance of the measurement wires and the surface temperature. b) Controller response to the targeted resistance change from 37°C to completely soft, completely rigid, completely flexible, and back to 37°C.

heating or cooling is required. If heating is needed, the supply voltage to the heating wires is adjusted, thereby regulating the current flow and associated joule heating. For cooling, the pump speed is regulated to give the associated volumetric cooling flow. Both heating current and pump speed are regulated with a PID controller. To avoid discontinuities when switching from heating to cooling and vice versa we implemented an activation threshold on both PID controllers. The controller does therefore take advantage of passive heating and cooling for small temperature and stiffness changes. Using the given required resistance change to rigidify or soften the catheter, the stiffness can be controlled by selecting the target resistance and controlling the heating and cooling of the catheter (Fig. 5b). The targeted resistance change can be reached quickly and accurately by heating or cooling.

### E. Experimental setup

Fig. 7 shows the experimental setup used to assess the controller performance, the transition times, and the magnetic actuation capabilities. The VSC is immersed in a water tank with a controlled temperature of 37°C. The water reservoir is placed in the workspace of a magnetic navigation system (Cardiomag [28]) while the water pumps and remaining control setup are placed in front of it.

## III. RESULTS

### A. Controller performance

To assess the controller performance, we analyzed its accuracy and speed given the required resistance change.

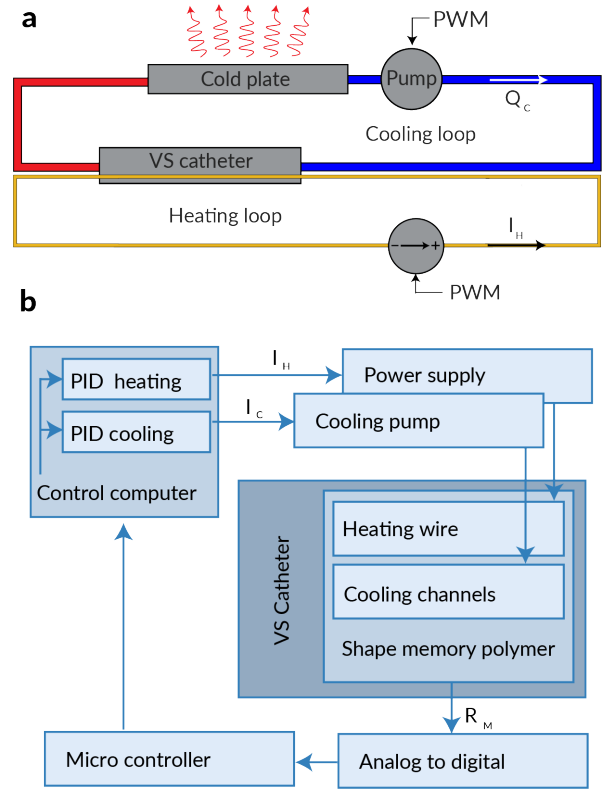


Fig. 6. Design of the hybrid stiffness control. a) Schematic illustration of the control setup with two separate loops for heating and cooling. Water is cooled with a cold plate and circulated with a peristaltic pump. Heat is generated in the heating wires with the application of an electric potential and associated current flow. b) Illustration of the controller design. The temperature of the SMP material is monitored and fed to a control computer. The controller evaluates whether heating or cooling is required and controls the power supply and cooling pump.

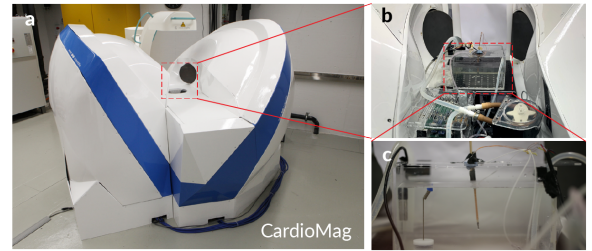


Fig. 7. Experimental setup. a) The Cardiomag, an electromagnetic navigation system is used to actuate the VSC. b) The water tank with a controlled temperature at 37°C is placed in the workspace of the Cardiomag. c) The catheter is placed in the water tank and actuated with an 80mT magnetic field.

Fig. 8 shows the bending radius of the VSC as a function of the measured resistance when the VSC is subjected to an externally generated magnetic field perpendicular to the catheter main axis. The magnetic field magnitude is set to 80mT while the surface temperature is controlled between 20°C and 45°C. The catheter, placed in a water tank at 37°C (Fig. 7), is incrementally cooled to the lowest setting ( $-0.15\Omega$ ) and heated back to the highest ( $0.075\Omega$ ) setting. This process has been repeated five times. The results



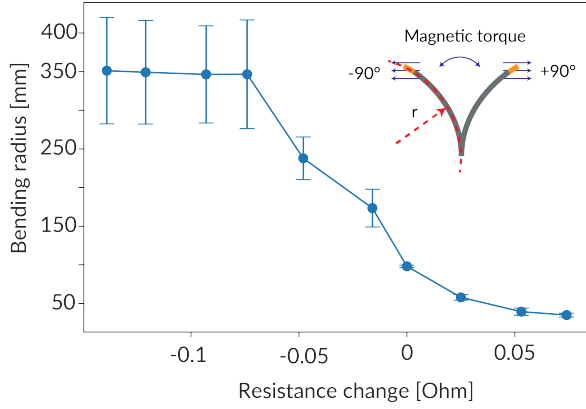


Fig. 8. Bending radius of the variable stiffness catheter upon application of a 80mT magnetic field as a function of temperature.

show an accurate and repeatable control of the tool temperature and associated stiffness. Additionally, we observed a stiffness variation that was predominantly restricted to the temperature range lower than  $37^{\circ}\text{C}$  (negative resistance change), thereby confirming the potentially increased safety of the VSC. Finally, a saturation on both ends indicates a stiffness/temperature control on the full stiffness range of the SMP material. The large relative errors in the rigid configuration (resistance change lower than  $-0.05\Omega$ ) are attributed to an asymmetric response to the magnetic field rotated by  $+90^{\circ}$  and  $-90^{\circ}$  with respect to the catheter main axis. The asymmetric behavior has been determined empirically.

### B. Transition time

The introduction of active heating and cooling drastically reduced the transition times from the flexible to the rigid state and vice versa with respect to passive heating or cooling. Passive heating and cooling refers to the uncontrolled state, thus relying on passive heat convection. Active heating and cooling refers to the controlled state as described above. The

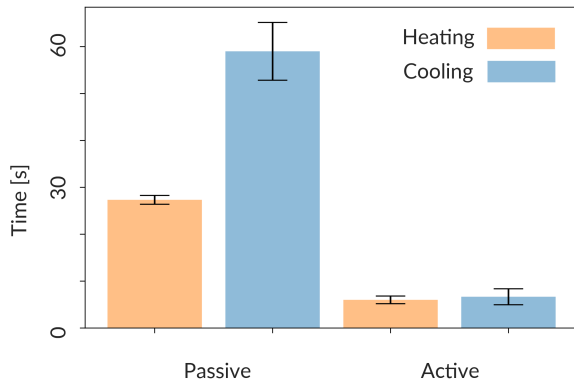


Fig. 9. Transition time from rigid to soft and vice versa. (left) Passively (natural convection) heated and cooled catheter compared to (right) actively (with heating and cooling) heated and cooled catheter.

transition times were analyzed with a catheter immersed in a  $37^{\circ}\text{C}$  warm water tank. The resistance (with its associated temperature) was recorded and used to assess the time required for each transition. As shown in Fig. 9, active heating and cooling reduces the transition times by more than a factor of five. Heating from the rigid (cold) state to  $37^{\circ}\text{C}$  is achieved in 6s instead of 27s without active heating. Cooling from the heated state to  $37^{\circ}\text{C}$  is achieved in 7s compared to 59s without active cooling. These high transition speeds allow for fast stiffness control without significant delays. Additionally, the asymmetric behavior of heated-only VSCs can be avoided. This highly benefits medical interventions as procedure times can be lowered while maintaining the benefits and accuracy of VS tools. These improvements also make the technology suitable for a broader range of applications in soft robotics allowing soft robots to rapidly change shape and lock their geometry.

### C. Controllable range

The proposed technology provides not only a large potential improvement with respect to safety and transition speed, but it also offers a broader material choice and larger stiffness transitions. Fig. 10 compares the controllable temperature range of the proposed catheter with that of the previously reported composite shape memory polymer catheter [20]. Without additional insulation layers, the heated catheter allows less than 30% of the stiffness transition to be used in endovascular applications (red range). The proposed catheter with hybrid control provides control of more than 90% of the full stiffness transition (blue and red range). Applications outside the endovascular field enable

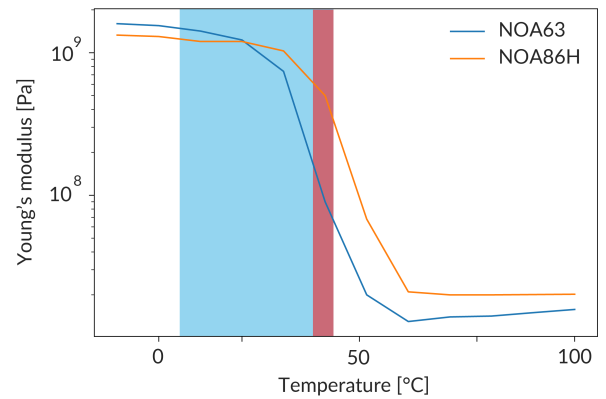


Fig. 10. Controllable stiffness range. Comparison between the heated NOA86H [20] variable stiffness catheter (red) and the proposed NOA63 catheter with hybrid stiffness control (blue).

larger temperature ranges, therefore affecting the allowed and controllable temperature and stiffness range. As reported in our previous work, endoscopic applications, for example, allow surface temperatures of up to  $51^{\circ}\text{C}$  for a brief period of time, therefore increasing the stiffness transition in both approaches to approximately 90% and 99%.

#### D. Magnetic actuation

The integration of the VSC into an electromagnetic navigation system allowed us to demonstrate the capabilities of the VSC. Fig. 11 shows the experimental validation of the hybrid VSC, demonstrating the ability to tune the tool's stiffness and steer the orientation of the catheter tip. The catheter, immersed in a 38°C water bath, can be bent by approximately 60° with a field of 80mT perpendicular

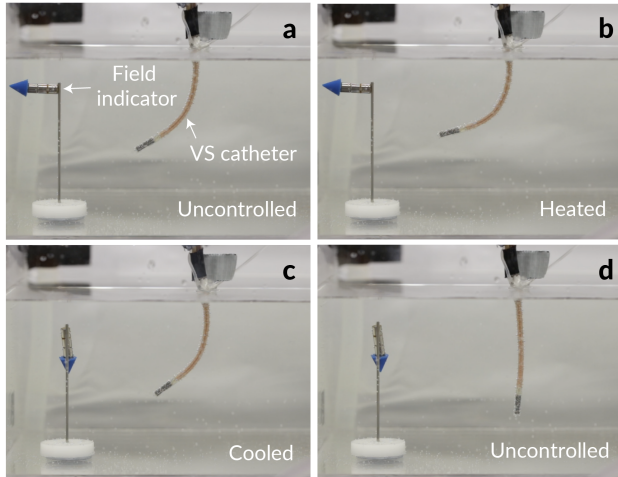


Fig. 11. Magnetic actuation of the variable stiffness catheter. a) Image of the VSC in the uncontrolled state (38°C) subjected to an 80 mT magnetic field rotated by 90° with respect to the catheter axis. b) Heated VSC subjected to the same magnetic field as in (a) c) Cooled VSC with a magnetic field oriented along the catheter main axis. d) VSC in the uncontrolled state in a field along the catheter main axis.

to the VSC proximal axis (Fig. 11a). Additional heating provides steerability enhancement by allowing a larger tip deflection of approximately 80° (Fig. 11b). By activating the cooling system, the shape of the catheter can be locked within seconds, guaranteeing a reliable force transmission between the proximal and distal end of the catheter. The deformed segment retains its shape upon the application of an 80mT magnetic field rotated by 90° (Fig. 11c). Finally, when switching off the controller, the catheter regains its flexibility and aligns with the magnetic field (Fig. 11d).

The integrated lumen provides a working channel for the insertion of tools, injections of liquids, integration of electrode connections, and camera cables both in the flexible and rigid configuration (Fig. 12a-d). The overall steerability and integration of a working channel provides a platform for additional medical applications.

#### IV. CONCLUSION

Our VS magnetic device provides a potentially significant increase in procedure safety and speed while maintaining scalability. This is highly beneficial for medical interventions as the procedure times can be lowered while maintaining the benefits and accuracy of VS tools. The biocompatible material with a glass transition temperature below body temperature provides potential safety in the case of failure of

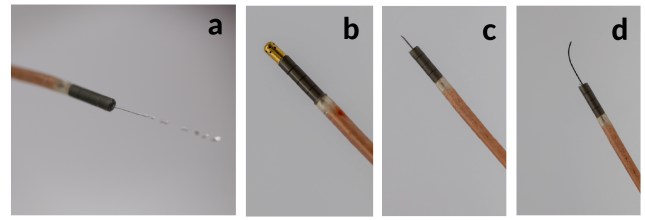


Fig. 12. Use of catheter lumen. a) The lumen is used to inject a liquid. b) An ablation electrode is integrated into the VSC. (c) The lumen is used to insert a 26 G needle. (d) A tool is inserted through the catheter lumen (demonstrated with a 0.0014 in guide wire).

the catheter and control system as the damaged tool can be retracted in the flexible configuration. Additionally, the lower surface temperature range guarantees no thermally induced tissue damage. The incorporation of cooling structures into the SMP material ensures scalability while providing control on the full stiffness range of the catheter. Hybrid control broadens the acceptable temperature range, increasing the selection of usable VS materials and allowing the use of the full stiffness spectrum for endovascular applications. The VS magnetic catheter can be selectively stiffened for improved stability and force transmission or softened for increased safety and dexterity. Additionally, the fast transition time opens a broader range of applications in the soft robotics field.

#### ACKNOWLEDGMENT

The authors would like to thank Francesco Briatico Van-gosa and Stefano Tagliabue from the Chemistry, Materials and Chemical Engineering department of Politecnico di Milano for their valuable support in the execution of the dynamic mechanical analysis of the shape memory polymers and the interpretation of the results, Yannick Armati for his help in the design of the cooling structures, and Elizabeth Zuurmond for correcting the manuscript. This work was supported by the Swiss National Science Foundation through grant numbers 200020B\_185039, by the ITC-InnoHK funding, and the ERC Advanced Grant 743217 Soft Micro Robotics (SOMBOT). SP and XC acknowledge funding from a Consolidator Grant (HINBOTS, Grant Agreement 771565).

#### REFERENCES

- [1] M. Runciman, A. Darzi, and G. P. Mylonas, "Soft Robotics in Minimally Invasive Surgery," *Soft Robotics*. [Online]. Available: <https://www.liebertpub.com/doi/pdf/10.1089/soro.2018.0136>
- [2] J. Burgner-Kahrs, D. C. Rucker, and H. Choset, "Continuum Robots for Medical Applications: A Survey," *IEEE Transactions on Robotics*, vol. 31, no. 6, pp. 1261–1280, dec 2015. [Online]. Available: <https://ieeexplore.ieee.org/document/7314984/>
- [3] Y. Kim, G. A. Parada, S. Liu, and X. Zhao, "Ferromagnetic soft continuum robots," *Science Robotics*, vol. 4, p. 7329, 2019.
- [4] M. Cianchetti, C. Laschi, A. Menciassi, and P. Dario, "Biomedical applications of soft robotics," *Nature Reviews Materials*, 2018.
- [5] A. Degani, H. Choset, A. Wolf, and M. Zenati, "Highly articulated robotic probe for minimally invasive surgery," in *Proceedings 2006 IEEE International Conference on Robotics and Automation, 2006. ICRA 2006*. IEEE, pp. 4167–4172. [Online]. Available: <http://ieeexplore.ieee.org/document/1642343/>

- [6] C. Chautems, S. Lyttle, Q. Boehler, and B. J. Nelson, "Design and Evaluation of a Steerable Magnetic Sheath for Cardiac Ablations," *IEEE Robotics and Automation Letters*, vol. 3, no. 3, pp. 2123–2128, 2018.
- [7] S. L. Charreyron, E. Gabbi, Q. Boehler, M. Becker, and B. J. Nelson, "A Magnetically Steered Endolaser Probe for Automated Panretinal Photocoagulation," *IEEE Robotics and Automation Letters*, vol. 4, no. 2, pp. 284–290, apr 2019.
- [8] C. de Marco, C. C. J. Alcántara, S. Kim, F. Briatico, A. Kadioglu, G. de Bernardis, X. Chen, C. Marano, B. J. Nelson, and S. Pané, "Indirect 3D and 4D Printing of Soft Robotic Microstructures," *Advanced Materials Technologies*, vol. 4, no. 9, p. 1900332, sep 2019. [Online]. Available: <https://onlinelibrary.wiley.com/doi/abs/10.1002/admt.201900332>
- [9] C. De Marco, S. Pané, and B. J. Nelson, "4D printing and robotics," *Science Robotics*, vol. 3, no. 18, pp. 2–4, 2018.
- [10] J. Lussi, M. Mattmann, S. Sevim, F. Grigis, C. De Marco, C. Chautems, S. Pané, J. Puigmartí-Luis, Q. Boehler, and B. J. Nelson, "A Submillimeter Continuous Variable Stiffness Catheter for Compliance Control," *Advanced Science*, vol. 8, no. 18, p. 2101290, sep 2021. [Online]. Available: <https://onlinelibrary.wiley.com/doi/full/10.1002/advs.202101290>
- [11] A. J. Loeve, P. Breedveld, and J. Dankelman, "Scopes too flexible and too stiff," *IEEE Pulse*, vol. 1, no. 3, pp. 26–41, 2010.
- [12] T. Yanagida, K. Adachi, and T. Nakamura, "Development of Endoscopic Device to Veer Out a Latex Tube with Jamming by Granular Materials," *Proceeding of the IEEE International Conference on Robotics and Biomimetics (ROBIO)*, no. December, pp. 1474–1479, 2013.
- [13] L. Blanc, A. Delchambre, and P. Lambert, "Flexible Medical Devices: Review of Controllable Stiffness Solutions," *Actuators 2017, Vol. 6, Page 23*, vol. 6, no. 3, p. 23, jul 2017.
- [14] M. Cianchetti, T. Ranzani, G. Gerboni, I. De Falco, C. Laschi, and A. Menciassi, "STIFF-FLOP surgical manipulator: Mechanical design and experimental characterization of the single module," *IEEE International Conference on Intelligent Robots and Systems*, pp. 3576–3581, 2013.
- [15] T. Ranzani, M. Cianchetti, G. Gerboni, I. D. Falco, and A. Menciassi, "A Soft Modular Manipulator for Minimally Invasive Surgery: Design and Characterization of a Single Module," *IEEE Transactions on Robotics*, vol. 32, no. 1, pp. 187–200, 2016.
- [16] F. Alambeigi, R. Seifabadi, and M. Armand, "A continuum manipulator with phase changing alloy," *Proceedings - IEEE International Conference on Robotics and Automation*, vol. 2016-June, pp. 758–764, jun 2016.
- [17] J. J. Abbott, E. Diller, and A. J. Petruska, "Magnetic Methods in Robotics," *Annual Review of Control, Robotics, and Autonomous Systems*, vol. 13, pp. 57–90, 2020.
- [18] C. Chautems, A. Tonazzini, D. Floreano, and B. J. Nelson, "A Variable Stiffness Catheter Controlled with an External Magnetic Field," *IEEE/RSJ International Conference on Intelligent Robots and Systems (IROS)*, sep 2017.
- [19] S. L. Charreyron, Q. Boehler, A. N. Danun, A. Mesot, M. Becker, and B. J. Nelson, "A Magnetically Navigated Microcannula for Subretinal Injections," *IEEE Transactions on Biomedical Engineering*, vol. 68, no. 1, pp. 119–129, jan 2021.
- [20] M. Mattmann, C. De Marco, F. Briatico, S. Tagliabue, A. Colusso, X. Z. Chen, J. Lussi, C. Chautems, S. Pané, and B. Nelson, "Thermoset Shape Memory Polymer Variable Stiffness 4D Robotic Catheters," *Advanced Science*, vol. 9, no. 1, p. 2103277, jan 2022. [Online]. Available: <https://onlinelibrary.wiley.com/doi/full/10.1002/advs.202103277>
- [21] L. Wang, Y. Yang, Y. Chen, C. Majidi, F. Iida, E. Askounis, and Q. Pei, "Controllable and reversible tuning of material rigidity for robot applications," *Materials Today*, vol. 21, no. 5, pp. 563–576, jun 2018. [Online]. Available: <https://www.sciencedirect.com/science/article/pii/S1369702117305618>
- [22] C. He, S. Wang, and S. Zuo, "A linear stepping endovascular intervention robot with variable stiffness and force sensing," *International Journal of Computer Assisted Radiology and Surgery*, vol. 13, pp. 671–682, 2018. [Online]. Available: <https://doi.org/10.1007/s11548-018-1722-x>
- [23] J. Liu, B. Hall, and M. Frecker, "Adjustable stiffness tubes via thermal modulation of a low melting point polymer Related content Compliant articulation structure using superelastic NiTiNOL," *Smart Mater. Struct*, vol. 21, p. 42001, 2012. [Online]. Available: <https://iopscience.iop.org/article/10.1088/0964-1726/21/4/042001/pdf>
- [24] J. Park, H. Lee, H. Kee, and S. Park, "Magnetically steerable manipulator with variable stiffness using graphene polylactic acid for minimally invasive surgery," *Sensors and Actuators A: Physical*, p. 112032, apr 2020. [Online]. Available: <https://www.sciencedirect.com/science/article/pii/S0924424720303150>
- [25] Y. Piskarev, J. Shintake, C. Chautems, J. Lussi, Q. Boehler, B. J. Nelson, and D. Floreano, "A variable stiffness magnetic catheter made of a conductive phase-change polymer for minimally invasive surgery," *Advanced Functional Materials*, p. 2107662, 2022.
- [26] H. M. Le, P. T. Phan, C. Lin, L. Jiajun, and S. J. Phee, "A Temperature-Dependent, Variable-Stiffness Endoscopic Robotic Manipulator with Active Heating and Cooling," *Annals of Biomedical Engineering*, vol. 48, no. 6, pp. 1837–1849, jun 2020. [Online]. Available: <https://link.springer.com/article/10.1007/s10439-020-02495-z>
- [27] S. S. Cheng, Y. Kim, and J. P. Desai, "Modeling and characterization of shape memory alloy springs with water cooling strategy in a neurosurgical robot," *Journal of intelligent material systems and structures*, vol. 28, no. 16, pp. 2167–2183, sep 2017.
- [28] S. Charreyron, "Remote magnetic navigation and applications in ophthalmic surgery," Ph.D. dissertation, ETH Zurich, Zurich, 2020. [Online]. Available: <https://doi.org/10.3929/ethz-b-000431062>